ELSEVIER

Journal of Materials Processing Technology 113 (2001) 109–114

Journal of Materials Processing Technology

www.elsevier.com/locate/jmatprotec

The influence of die geometry on the radial extrusion processes

Beong Du Ko*, Dong Joon Kim, Soo Hyung Lee, Boeng Bok Hwang

Department of Industrial Automation Engineering, Inha University, 253 Yonghundong, Inchon, South Korea

Abstract

Three variants of radial extrusion are analyzed by simulation work. Case I involves forcing a cylindrical billet against a flat die. In case II, the upper punch forces a billet against a stationary punch recessed in the lower die. In case III, both the upper and lower punches move together toward the center of the billet. Major process parameters are identified as the relative gap height and the die corner radius in constant relative deformation. The simulation work is performed by the rigid–plastic finite element method. The validity of the modeling and simulation work for this process is verified by comparison with experimental data in terms of forming load. The simulation results show good agreement with the experimental data. Based on the simulation results, the different process parameters are related to the different material flow. Due to various die motions, a certain pattern in the material flow is shown in each deformation case. The die geometry has a significant influence on the material flow into the flange gap.

Keywords: Radial extrusion; Rigid–plastic FEM; Relative gap height; Die corner radius; Die geometry

1. Introduction

The basic processes involved in cold extrusion are classified depending on their forming direction as forward, backward, and radial or lateral extrusion. In these processes, radial extrusion is a forming process in which one or two opposed punches move axially causing radial flow into the die cavity or into an annular space. The initial billet can be cylindrical solid as well as tubular. Components featuring a central hub with complex flange geometry, such as tube fittings or differential gears, are typical parts that can be produced advantageously by radial extrusion, without the need of secondary machining operations [1].

The process of radial extrusion has been studied by many process designers by extensive experimental work or finite element simulation [1–6]. Extensive experimental work performed by Andersen and Andersen [2] led to the operational limits and revealed the existence of four different modes of deformation in the radial extrusion of tubes. Also, Schätzle [3] in his experimental work determined operational limits for AISI 1006 in radial extrusion of cylindrical solid billet with double acting tool.

In the radial extrusion of a solid cylindrical billet, the major process parameters are identified as the ratio of gap height to billet diameter (relative gap height), the die corner radius and the ratio of stroke to billet diameter (relative deformation). Referring to the operational limits by Schätzle, when the relative deformation is 125% and the relative gap height is less than 0.25 mm/mm, cracks were observed which propagated from the flange edge to the shank due to large tangential stress. Also, annular folding occurred, when the relative gap height was greater than 1.4 mm/mm [3].

In this paper, the material flow into the flange gap in three variant radial extrusions of a solid cylindrical billet is analyzed by extensive finite element simulation work. The major process parameters considered in this work are the relative gap height and the die corner radius. Several different values of parameters are selected within the operational limits to analyze the effect of the process parameters on the material flow. The analysis procedure is as follows: firstly, the results of simulation performed under the same conditions as for experiment are compared with experimental data [5] in terms of forming load. This comparison is to verify the validity of the rigid–plastic finite element method. Secondly, extensive simulation work for various combinations of parameter value was performed, and then the main characteristics of the deformation patterns of each case are observed to define the terms which represent the forming characteristic of the flange. Thirdly, the effects of major parameters on the material flow into the flange gap are analyzed.

The main objective of this study is the analysis of the influence of geometrical parameters, such as relative gap height and die corner radius, on the material flow into the flange gap.

* Corresponding author.

0924-0136/01/$ – see front matter
PII: S0924-0136(01)00704-X

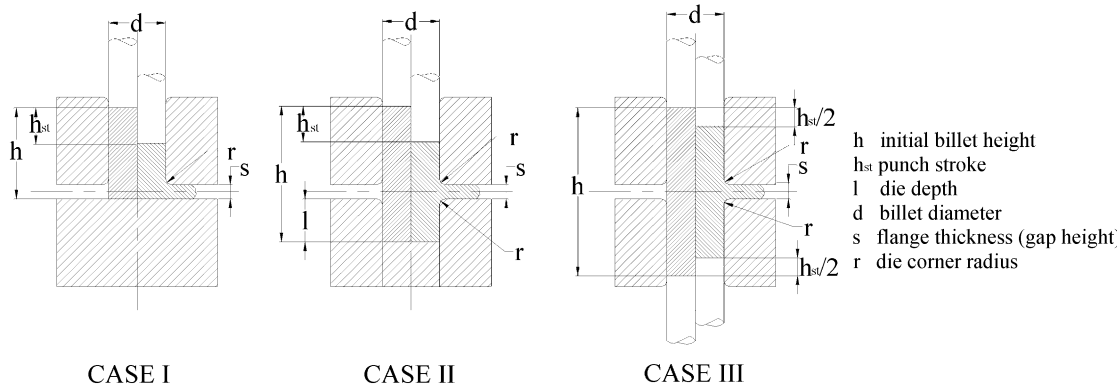

Fig. 1. The die geometry of radial extrusion.

2. Analysis of radial extrusion

The deformation patterns of radial extrusion and the influence of major geometrical parameters on the process are analyzed by the rigid–plastic finite element method.

2.1. The geometrical parameters in radial extrusion

This work investigates three basic variants of radial extrusion, as shown in Fig. 1. The figure shows the principle of these processes and the geometrical parameters utilized in this work.

Case I involves forcing of a cylindrical billet by a punch against a flat die which is stationary. In case II, an upper punch forces a billet against a stationary punch recessed in the lower die. In case III, both upper and lower punches move together toward the center of the billet. The initial billet and the final product are shown in Fig. 1. The major process parameters are identified as the relative gap height (s/d), the relative deformation (h_{st}/d), and the die corner radius (r) [5].

To investigate the influence of relative gap height (s/d) and die corner radius (r) on the material flow, finite element analysis is performed for different values of gap height (s) and die corner radius (r) selected within the operational limits. The other parameters such as punch stroke (h_{st}), initial billet diameter (d), billet height (h), and die depth (l) are the same in each case. Constant relative deformation (h_{st}/d) means that the volume of material extruded into the flange is constant. The specific values of the geometrical parameters are summarized in Table 1. Twenty different simulations were performed in the case I process, 16 in case II, and 20 in case III.

2.2. The finite element analysis

The process is simulated by the rigid–plastic finite element code ALPID [7]. The material employed in the simulation is AISI 1006 steel. The flow stress–strain relationship of this material at room temperature can be modeled as Eq. (1) [8]. The friction factor at the die–material interface is assumed to be 0.1 in the cold forging of steels, using conventional phosphate-soap lubricants or oil [9].

$$\bar{\sigma} = 62.9\bar{\varepsilon}^{0.31}\ \mathrm{kgf/mm^2} \quad (1)$$

3. Results and discussion

In the following sections, the results of the FE simulation are given and discussed for investigating the influence of the major parameters on the material flow. Firstly, the validity of the modeling and simulation work for this process are investigated, and then the deforming pattern of each case

Table 1
Geometrical parameters used in process analysis

	Case I	Case II	Case III
Initial billet height (h)	50.0 mm	66.0 mm	100.0 mm
Die depth (l)	–	16.0 mm	–
Billet diameter (d)	16.0 mm	16.0 mm	16.0 mm
Punch stroke (h_{st})	20.0 mm	20.0 mm	20.0 mm
Relative deformation (h_{st}/d)	125 mm/mm	125 mm/mm	125 mm/mm
Gap height (s)	4.0, 5.0, 6.0, 8.0 mm	6.0, 8.0, 10.0, 12.0 mm	4.0, 8.0, 12.0, 16.0 mm
Relative gap height (s/d)	0.25, 0.31, 0.38, 0.50 mm/mm	0.38, 0.50, 0.63, 0.75 mm/mm	0.25, 0.50, 0.75, 1.0 mm/mm
Die corner radius (r)	1.0, 2.0, 3.0, 4.0, 5.0 mm	2.0, 3.0, 4.0, 5.0 mm	1.0, 2.0, 3.0, 4.0, 5.0 mm
Number of combination	20	16	20

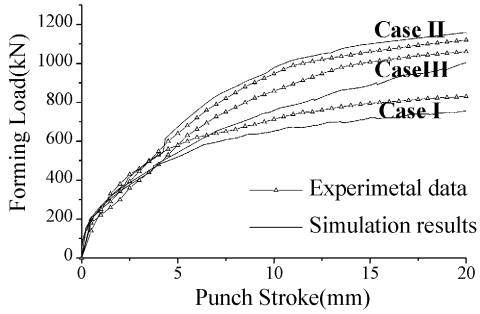

Fig. 2. Comparison of the simulated and experimental curve of forming load [5] for $s/d = 0.25$, $r = 5$ mm and $d = 32.0$ mm.

is discussed. Especially, the influences of the relative gap height (*s*/*d*) and die corner radius (*r*) on the deforming patterns are analyzed quantitatively.

3.1. Comparison with experiment

To verify that the modeling and simulation work for this process are valid, the load–stroke relationships obtained by FE simulation are compared with the experimental data in reference [5]. Both simulation and experiment were performed under the same conditions of relative gap height $s/d = 0.25$, die corner radius $r = 5$ mm, billet diameter $d = 32.0$ mm, for AISI 1006 steel. Fig. 2 shows the load–stroke curves of simulation and experiment [5] for three different cases. The curve shapes of the simulation results are similar to those of the experimental data, the difference between them being within less than 10%. This comparison shows reasonably good agreement between FE simulation and experiment.

In addition, considering the forming load of the three cases, case I requires the least load because most of the die–material interface is lubricated, while the other two cases feature more internal shear. For cases II and III, case II requires greater load than case III due to asymmetrical material flow [5].

3.2. The deformation patterns

The representative deformation patterns of each case are shown in Fig. 3. The left half of each figure represents the ideal forming shape, but the actual deformation shape obtained from the FE simulation shows asymmetric and unsound forming patterns, as shown in the right half figure. The details of the deformation patterns of the flange are shown in circles in the figure.

In case I, the edge of the flange is separated from the lower die under a certain condition. The upper figure of case I shows this phenomenon for $s/d = 0.31$ and $r = 3$ mm, but the edge of the flange is not separated for $s/d = 0.38$ and $r = 5$ mm, as shown in the lower figure. To investigate the influence of parameters on this edge-separation, the height from the flat die to the edge of flange is defined as the separation height, h_G.

The case II deformation causes asymmetrical material flow into the flange gap. To investigate the degree of asymmetry for *s*/*d* and *r*, the asymmetric ratios of height and angle are defined as h_U/h_D and α_U/α_D, respectively. As

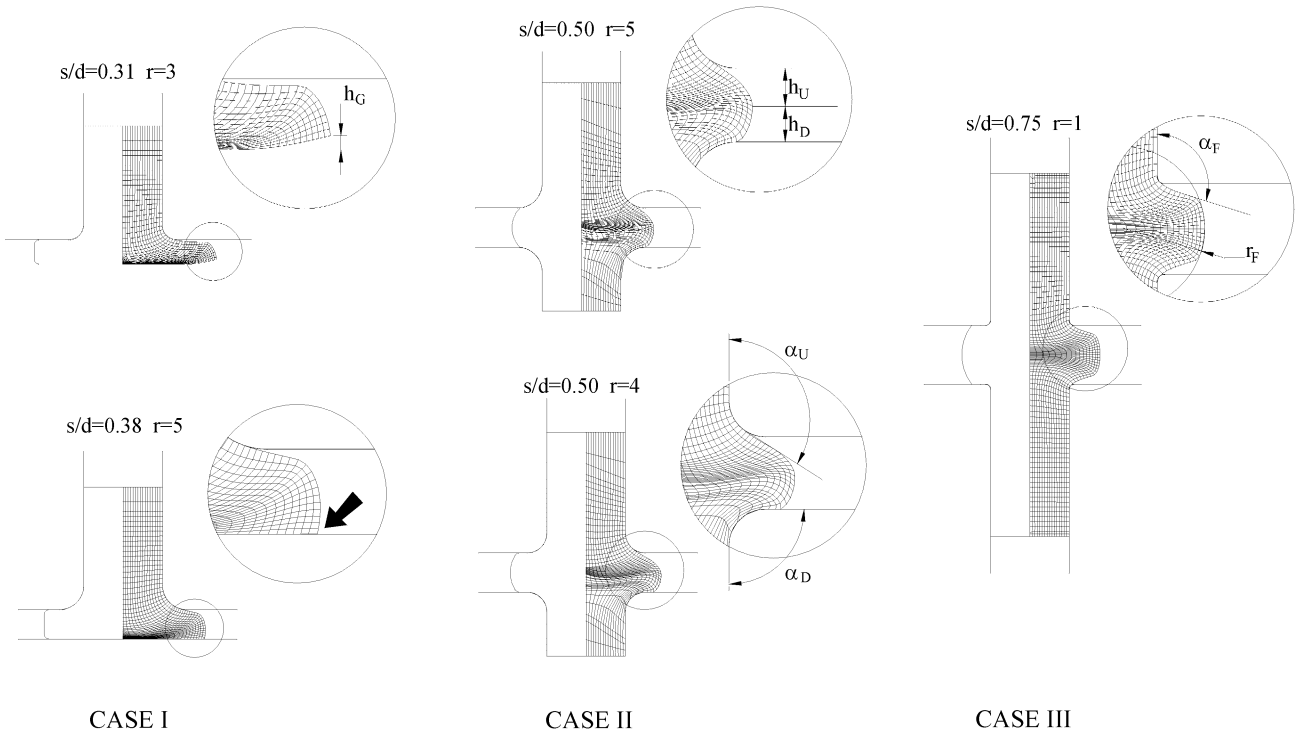

Fig. 3. Deformation patterns of the three variant processes for various values of *s*/*d* and *r* with friction factor $m = 0.1$.

indicated in the upper figure of case II, h_U and h_D are the height from the top of flange in the radial direction to the upper die surface and to the lower die surface, respectively, and α_U and α_D are the upper and lower flange angle as indicated in the lower figure of case II, respectively.

In case III, the material flows into the gap at some angle to the horizontal die surface. Also the flange radius varies with *s/d* and *r*. Therefore, the flange angle and the flange radius are defined as r_F and α_F as shown in Fig. 3. Then the influence of *s/d* and *r* on r_F and α_F is investigated, respectively.

3.3. The influences of die geometry

The influence of the major parameters on the important deformation characteristics in each deformation case is given quantitatively and discussed in this section. The major parameters are the relative gap height (*s/d*) and die corner radius (*r*) for constant relative deformation (h_{st}/d). The important deformation characteristics are the separation height (h_G) in case I, the asymmetric ratios of height and flange angle (h_U/h_D and α_U/α_D) in case II and the flange radius (r_F) and flange angle (α_F) in case III, as defined earlier.

3.3.1. Case I: one die against a level tool surface

In case I, the edge of the flange is separated from the lower plate die under a certain condition. Fig. 4 illustrates the variation of the separation height (h_U) under the condition when the relative deformation is kept constant (h_{st}/d) and the relative gap height (*s/d*) and die corner radius (*r*) are varied. Under the condition of $s/d = 0.25$ and $r = 1, 2$ and 3 mm, the edge of the flange is separated during processing and then the upper portion of the flange touches the upper die surface. In this case, the edge-separation is constrained by the upper die. Therefore, these data are excluded in the analysis.

As seen in Fig. 4, the separation height (h_G) decreases, as the relative gap height (*s/d*) increases from $s/d = 0.25, 0.31$, 0.38 to 0.50. Especially, the separation height (h_G) turns out to be zero for $s/d = 0.50$ with all corner radius. For constant *s/d*, the separation height (h_G) decreases as the die corner radius (*r*) increases from $r = 1, 2, 3, 4$ to 5 mm. These results show that both the large relative gap height (*s/d*) and die corner radius (*r*) lead to the separation height (h_G) being smaller on zero.

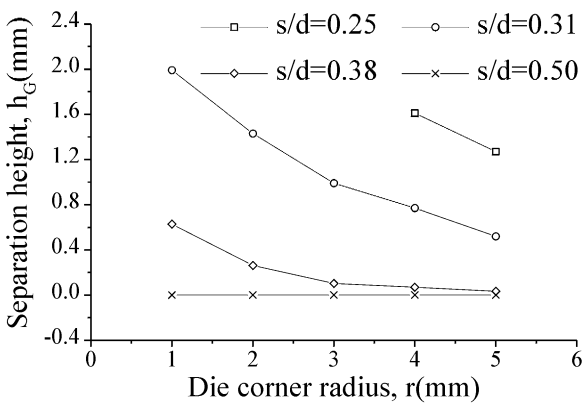

Fig. 4. Effect of die corner radius (*r*) on the separation height (h_G) for relative gap height (*s/d*).

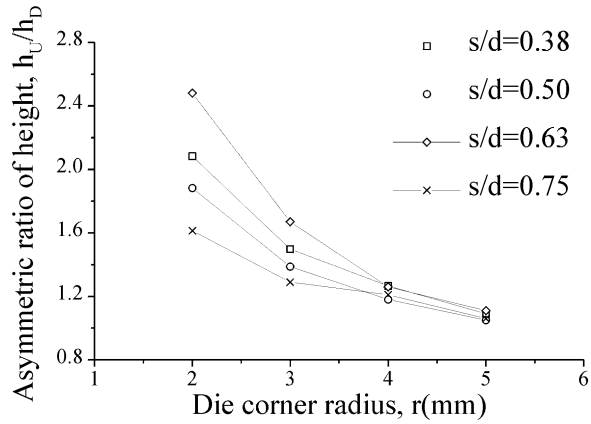

Fig. 5. Effect of die corner radius (*r*) on the asymmetric ratio of height (h_U/h_D) for relative gap height (*s/d*).

3.3.2. Case II: one die against a solid counter-die

Asymmetrical material flow is the major characteristic in case II deformation. Fig. 5 shows the effect of die corner radius (*r*) on the asymmetric ratio of height (h_U/h_D) for relative gap height (*s/d*). A greater relative gap height (*s/d*) dose not always lead to a larger ratio of h_U/h_D. At the intermediate value of $s/d = 0.63$, the ratio of h_U/h_D has greatest value. However, the ratio of h_U/h_D decreases from the maximum, 2.48, to the minimum, 1.05, as the die corner radius increases from 2 to 5 mm. This result shows that the corner radius (*r*) is a dominant parameter for the ratio of h_U/h_D and that a large die corner radius reduces the ratio of h_U/h_D.

Fig. 6 shows the effect of die corner radius (*r*) on the ratio of α_U/α_D for relative gap height (*s/d*). It is observed from the

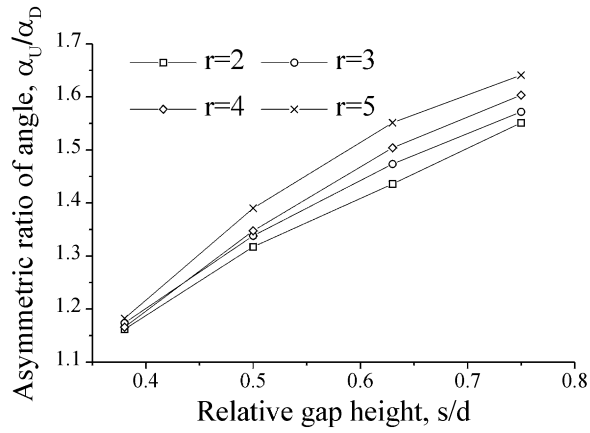

Fig. 6. Effect of relative gap height (*s/d*) on the asymmetric ratio of angle (α_U/α_D) for die corner radius (*r*).

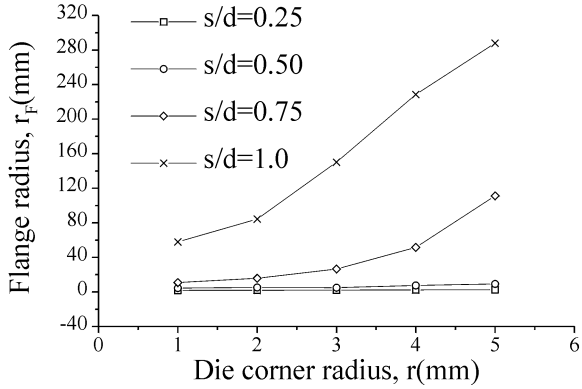

Fig. 7. Effect of die corner radius (r) on the flange radius (r_F) for different relative gap height (s/d).

figure that as relative gap height (s/d) and die corner radius (r) increases, the ratio of α_U/α_D also increases. However, the effect of relative gap height (s/d) is more significant than that of die corner radius. When the relative gap height (s/d) increases by 97% from $s/d = 0.38$ to 0.75, the ratio of α_U/α_D shows an increase of 39% for $r = 5$ mm, whereas the ratio of α_U/α_D increases only by 8.4% for a 150% increase of die corner radius (r) from $r = 2$ to 5 mm, when $s/d = 0.63$.

3.3.3. Case III: counter-operating die

In case III deformation, mainly the flange shape in terms of flange radius (r_F) and flange angle (α_F) is considered. Fig. 7 illustrates the effect of die corner radius (r) on the flange radius (α_F) for different relative gap height (s/d). When the relative gap height (s/d) is small, the effect of die corner radius (r) is not significant. However, the effect of die corner radius (r) becomes significant with increase of relative gap height (s/d). For a relative gap height (s/d) of 1.0, the flange radius (r_F) shows an increase of 397% when the die corner radius (r) increases from 1 to 5 mm.

Fig. 8 illustrates the variation of the flange angle (α_F) with die corner radius (r) for different relative gap height (s/d). It is observed from the figure that the relative gap height (s/d)

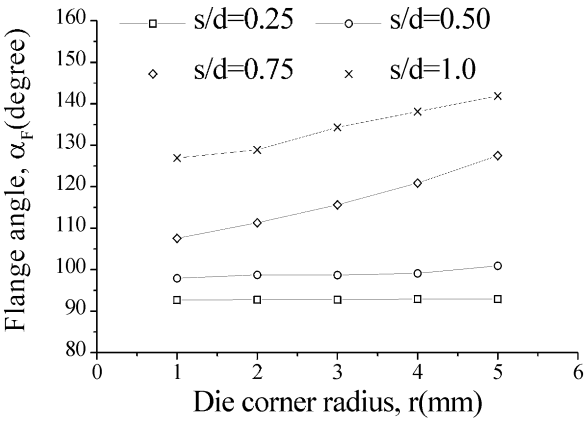

Fig. 8. Effect of die corner radius (r) on the flange angle (α_F) for relative gap height (s/d).

has a more significant effect than the die corner radius (r) on the flange angle (α_F). For a constant relative gap height (s/d) of 0.75, the flange angle (α_F) shows an increase of about 18.6% when die corner radius (r) increases by 400% from 1 to 5 mm. However, the flange angle (α_F) increases in 52.8%, when the relative gap height (s/d) increases in 300% from 0.25 to 1.0 for a constant die corner radius of 5 mm.

From the results shown in Figs. 6 and 7, it can be seen that the dominant geometric parameter influencing the flange radius (r_F) is the die corner radius (r), while the relative gap height (s/d) is a dominant parameter influencing the flange angle (α_F).

3.4. The effect of friction factor on the separation height

In case I deformation, it is expected that the edge-separation might be related with the condition of the die–material interface. Thus, the effect of the friction condition on the separation height (h_G) is analyzed. FE simulation under the additional condition of three different friction factors, $m = 0.1$, 0.2, 0.3, was performed, when $s/d = 0.50$ and $r = 5$ mm. The results show that the flange is extruded with

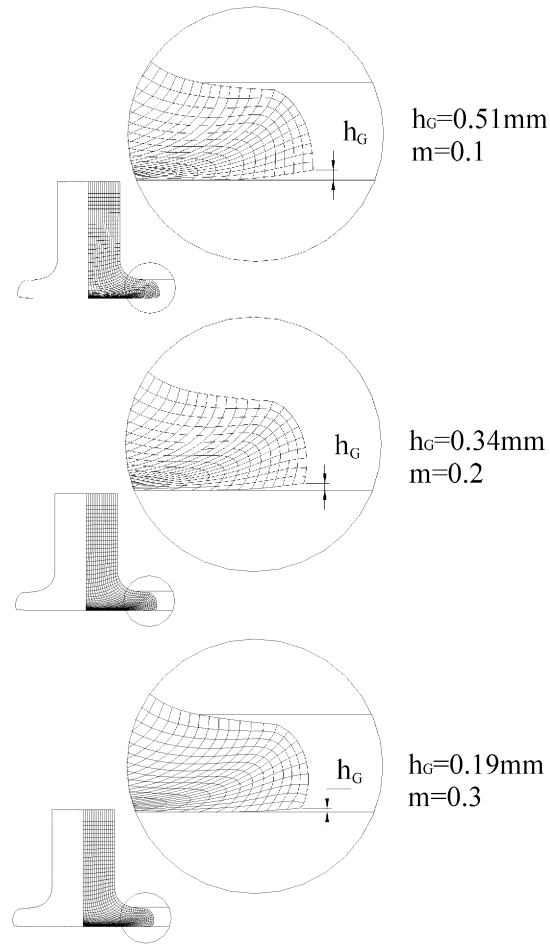

Fig. 9. Effect of friction factor on the separation height (h_G) for $s/d = 0.50$ and $r = 5$ mm.

smaller separation height (h_G), as the friction factor (m) increases from $m = 0.1$ to 0.3, as shown in Fig. 9. From this result, it is concluded that a higher friction disturbs the material flow at the lower die interface and this leads to the lower separation height (h_G).

4. Conclusions

The influence of die geometry on the radial extrusion process is analyzed by the rigid–plastic FEM. The main parameters in die geometry are the relative gap height (s/d) and the die corner radius (r). The material flow into the flange gap in the three cases of radial extrusion is analyzed extensively. Throughout the finite element analysis for various combinations of geometrical parameters, the following conclusions are obtained.

1. A large relative gap height (s/d) and die corner radius (r) lead separation height (h_G) to be lower or zero in case I.
2. The flange is extruded with a smaller separation height (h_G), when the friction between the lower die and the material is greater in case I.
3. The die corner radius (r) is a dominant parameter influencing the ratio of h_U/h_D, and a large corner radius (r) reduces the ratio of h_U/h_D in case II.
4. The ratio of α_U/α_D increases, as the relative gap height (s/d) and the die corner radius (r) increase. However, the effect of s/d is more significant than that of die corner radius (r) in case II.
5. The flange radius (r_F) increases, as die corner radius (r) increases. The effect is more significant when s/d is large in case III.
6. The large relative gap height (s/d) and die corner radius lead to large flange angle (α_F). However, the relative gap height (s/d) is a dominant parameter in case III.

With this effect of die geometry considered, it is concluded that the material flow into the flange gap in radial extrusion can be controlled by adjusting the geometrical parameters within the design limits.

Acknowledgements

This work was supported by the development program for the exemplary schools in information and communication from the Ministry of Information and Communication (MIC) and an RA research grant from Inha University.

References

[1] S.B. Petersen, R. Balendra, J.M.C. Rodrigues, P.A.F. Martins, J. Mater. Process. Technol. 69 (1997) 155.
[2] B. Andersen, C.B. Andersen, Radial extrusion of tubular components, MM 91.27, M.Sc. Thesis, Institute of Manufacturing Engineering, Technical University of Denmark, 1991.
[3] W. Schätzle, Radial extrusion of flanges on steel cylindrical workpieces (in German), Technical Report 93, Institute for Metal Forming, University of Stuttgart, Springer, Berlin, 1987.
[4] W. Schätzle, Wire 34 (2) (1984) 71.
[5] J.A. Pale, R. Shivpuri, T. Altan, Development of equipment and capabilities for investigation of the multi-action forming of complex parts, Engineering Research Center for Net Shape Manufacturing, Ohio State University, 1989.
[6] M. Arentoft, H. Bjerregaard, C.B. Andersen, T. Wanheim, J. Mater. Process. Technol. 75 (1998) 122.
[7] S.I. Oh, G.D. Lahoi, T. Altan, ALPID — a general purpose FEM program for metal forming, Proceedings of the NAMRC IX, State College, Pennsylvania, 1981.
[8] J.R. Douglas, T. Altan, A study of mechanics of closed-die forging, phase II, Final Report, Battelle's Columbus Laboratories, Columbus, OH, Contract DAAG46-71-C-0095, 1972.
[9] S. Kobayashi, S.I. Oh, T. Altan, Metal Forming and the Finite Element Method, Oxford University Press, New York, 1989.